J|A|C|S
ARTICLES
Published on Web 08/23/2002

A High-Throughput Optical Screening Method for the Optimization of Colloidal Water Oxidation Catalysts

Natalie D. Morris and Thomas E. Mallouk*

Contribution from the Department of Chemistry, The Pennsylvania State University, University Park, Pennsylvania 16802

Received December 28, 2001

Abstract: A high-throughput method has been developed for screening and optimization of colloidal water oxidation catalysts. The catalysts are irradiated in parallel by visible light from an overhead projector in solutions containing tris(2,2′-bipyridyl)ruthenium(II) ($Ru(bpy)_3^{2+}$) and persulfate. The array of reaction solutions is held in a 96-well plate, and absorbance readings are taken intermittently using a bioassay plate reader. The absorbance at 430 nm is indicative of the amount of $Ru(bpy)_3^{2+}$ remaining in solution. The best catalysts give the most persistent absorbance, because the oxygen evolution reaction is kinetically competitive with decomposition of $Ru(bpy)_3^{3+}$. Reagent concentrations were varied using a factorial design-of-experiment approach in order to optimize reaction conditions for a $IrO_2 \cdot xH_2O$ colloidal catalyst. A higher colloid concentration, a lower $Ru(bpy)_3^{2+}$ concentration, and a higher pH buffer doubled the number of turnovers relative to the original conditions. Metal oxide colloids consisting of $IrO_2 \cdot xH_2O$ doped with varying amounts of Pt, Ru, and Os were made using a parallel microwave synthesis technique and were tested both by the parallel screening method and by direct measurement of oxygen evolution. The correlation between the two methods was good, with Ir−Pt−Os oxide compositions showing the highest activity. The effect of adding small amounts of Pt and Os to $IrO_2 \cdot xH_2O$ appears to be predominantly to reduce the particle size of the colloids.

Introduction

Photochemical water splitting is one of the most attractive potential means of converting sunlight to usable chemical energy. In principle, light of both visible and near-infrared wavelengths is sufficiently energetic to drive the water-splitting reaction. However, the search for a robust and efficient photocatalyst for this reaction has been very challenging. The problem has been actively pursued for approximately 30 years,[1] and only recently has the first visible light water-splitting catalyst (Ni-doped $InTaO_4$) been reported.[2] While this is an important milestone in the field, the efficiency is low, and it is not immediately apparent how one could improve upon the visible light absorbing metal oxides that have been tested so far as photocatalysts.[3−6]

Another approach to the problem is to design composite systems that consist of molecular photosensitizers coupled to colloidal or solid catalysts.[7−11] In this case the problem is simplified by studying the hydrogen and oxygen half-reactions separately. The catalysts and reaction conditions are optimized for each in the hope of combining them for the overall water-splitting reaction. One of the difficulties in this work has been the search for oxygen-evolving catalysts.[12] Harriman et al. studied a variety of metal oxide powders, using tris(2,2′-bipyridyl)ruthenium(II) ($Ru(bpy)_3^{2+}$) as the photosensitizer, and found the highest rates of oxygen evolution with IrO_2 and Co_3O_4. Other powders that performed moderately well included RuO_2, Rh_2O_3, Mn_2O_3, and $NiCo_2O_4$.[13] Among colloidal catalysts, $IrO_2 \cdot xH_2O$[14] and $RuO_2 \cdot 2H_2O$[15] have been the most thoroughly studied. However, $RuO_2 \cdot 2H_2O$ is unstable under photochemical conditions. The highest quantum yields and number of turnovers for oxygen evolution from $Ru(bpy)_3^{2+}$, using persulfate as a sacrificial electron acceptor, have been achieved using $IrO_2 \cdot xH_2O$.[16]

In general, the photochemical oxygen evolution half reaction is carried out as shown in Scheme 1. A sensitizer molecule or polymer ($Ru(bpy)_3^{2+}$ is shown here as the most widely used

* Address correspondence to this author. E-mail: Tom@chem.psu.edu.

(1) Fujishima, A.; Honda, K. *Nature* **1972**, *37*, 238.
(2) Zou, Z.; Ye, J.; Sayama, K.; Arakawa, H. *Nature* **2001**, *414*, 625.
(3) Takata, T.; Tanaka, A.; Hara, M.; Kondo, J. N.; Domen, K. *Catal. Today* **1998**, *44*, 17.
(4) Yoshimura, J.; Ebina, Y.; Kondo, J.; Domen, K.; Tanaka, A. *J. Phys. Chem.* **1993**, *97*, 1970.
(5) Tokunaga, S.; Kato, H.; Kudo, A. *Chem. Mater.* **2001**, *13*, 4624.
(6) Kudo, A.; Mikami, I. *Chem. Lett.* **1998**, 1027.
(7) Kiwi, J.; Grätzel, M. *J. Am. Chem. Soc.* **1979**, *101*, 7214.
(8) Brugger, P. A.; Cuendet, P.; Graetzel, M. *J. Am. Chem. Soc.* **1981**, *103*, 2923.
(9) Miller, D.; McLendon, G. *Inorg. Chem.* **1981**, *20*, 950.
(10) Kim, Y.; Salim, S.; Huq, M.; Mallouk, T. E. *J. Am. Chem. Soc.* **1991**, *113*, 9561.
(11) (a) Kim, Y.; Atherton, S. J.; Brigham, E. S.; Mallouk, T. E. *J. Phys. Chem.* **1993**, *97*, 11802. (b) Saupe, G. B.; Kim, W.; Schmehl, R. H.; Mallouk, T. E. *J. Phys. Chem. B* **1997**, *101*, 2508.
(12) Harriman, A. *Platinum Met. Rev.* **1984**, *27*, 102.
(13) Harriman, A.; Pickering, I. J.; Thomas, J. M.; Christensen, P. A. *J. Chem. Soc., Faraday Trans. 1* **1988**, *84*, 2795.
(14) Harriman, A.; Thomas, J. M.; Millwood, G. R. *New J. Chem.* **1987**, *11*, 757.
(15) Harriman, A.; Richoux, M. C.; Christensen, P. A.; Mosseri, S.; Neta, P. *J. Chem. Soc., Faraday Trans. 1* **1987**, *83*, 3001.
(16) Hara, M.; Waraksa, C. C.; Lean, J. T.; Lewis, B. L.; Mallouk, T. E. *J. Phys. Chem. A* **2000**, *104*, 5275.

10.1021/ja017895f CCC: $22.00

Scheme 1. Photocatalytic Water Oxidation Cycle Using $Ru(bpy)_3^{2+}$ as the Sensitizer in a Sacrificial Electron Acceptor System

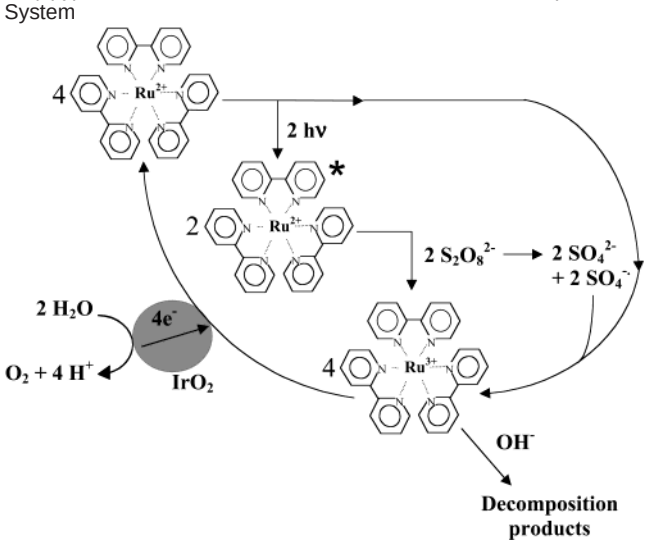

example) absorbs visible light. In the case of $Ru(bpy)_3^{2+}$, a metal-to-ligand charge-transfer (MLCT) excited state is formed.[17] The MLCT state is quenched by reaction with persulfate ion ($S_2O_8^{2-}$), forming $Ru(bpy)_3^{3+}$, $SO_4^{-\bullet}$, and SO_4^{2-}. In the absence of a catalyst, $Ru(bpy)_3^{3+}$ rapidly and irreversibly decomposes to inactive products, and the solution turns colorless.[16] On the surface of a suitable catalyst, however, oxygen is evolved, and the reduced form of the sensitizer is regenerated. After four turnovers of the $Ru(bpy)_3^{2+/3+}$ couple, which requires two photons in this sacrificial system, one molecule of O_2 is produced.

Under optimized conditions, the quantum efficiency of photochemical oxygen evolution from $IrO_2 \cdot xH_2O$, as shown in Scheme 1, can exceed 70%. While this sounds impressive, substantial improvement in the colloidal catalyst is needed for two reasons. First, the photosensitizer survives for, at best, a few hundred turnovers before it is decomposed by nucleophilic attack of water or OH^- on $Ru(bpy)_3^{3+}$. Because this reaction occurs in competition with hole transfer from $Ru(bpy)_3^{3+}$ to the colloidal catalyst, it follows that a better catalyst will increase the lifetime of the sensitizer. Second, the oxygen-evolving reaction should outpace any charge-recombination reactions that occur in a full (nonsacrificial) water-splitting cycle. Typically, charge recombination occurs on a microsecond to millisecond time scale in molecular and dye/semiconductor donor−acceptor systems.[18−23]

The search for better oxygen evolution catalysts is complicated by the many factors that influence the reaction kinetics. Apart from the composition of the colloidal catalyst itself, the method of colloid preparation, as well as the presence of different buffers, stabilizers, and supports, all affect the catalyst turnover rate. Decomposition of the sensitizer occurs more rapidly if the sensitizer molecules are not in physical contact with the catalyst, or if the catalyst itself is not efficient at reducing the oxidized form of adsorbed sensitizer molecules. To date, these factors have been optimized empirically and in a serial fashion. Catalysts are tested by continuous photolysis, in which oxygen evolution is monitored by periodically withdrawing headspace samples and analyzing them by gas chromatography (GC). This process takes 1−2 h per sample and is unwieldy for comparison of large numbers of catalysts because it requires, for each one, a steady light source, a reaction vessel purged with inert gas (to eliminate interference from atmospheric O_2), and frequent GC injections. If serial tests are performed on different days, then fresh colloids and buffers must be prepared, and this introduces another source of error in the comparison.

One of the most convenient ways of adapting a catalysis problem to rapid, parallel screening is to detect the products or byproducts of the reaction optically, as a change in absorbance or emission.[24−30] We report here a new parallel, high-throughput method for testing large numbers of colloidal oxygen-evolving catalysts. The method uses optical, indirect detection of the reaction and is based on the idea that sensitizer turnover/sensitizer decomposition represents a kinetic branch point in Scheme 1. The method—which involves detecting the absorbance or emission of residual $Ru(bpy)_3^{2+}$—relies on the fact that poorer catalysts give more rapid decomposition of the sensitizer, because the catalytic cycle is not kinetically competitive with nucleophilic attack on $Ru(bpy)_3^{3+}$. Because oxygen is not detected directly, the requirement for a sealed, inert-gas-filled reaction vessel is removed. As an optical method, it also avoids interferences associated with electrochemical detection of reaction products.[31] When the reaction volume is scaled down to a microwell format, then an entire array of catalysts can be irradiated simultaneously (using light from an overhead projector) and periodically interrogated during the photolysis by means of an automated plate reader. We show here that this method allows one to optimize, in a rapid and straightforward manner, both the reaction conditions and the composition of colloidal catalysts for photochemical oxygen evolution.

Experimental Section

Conventional Synthesis of Colloidal $IrO_2 \cdot xH_2O$.[16] A 6.2×10^{-4} M colloidal $IrO_2 \cdot xH_2O$ solution was made by adding 0.3 g of K_2IrCl_6 to a 50 mL aqueous solution of 0.5 g of sodium hydrogen citrate sesquihydrate. The solution pH was adjusted to 7.0 using 0.25 M NaOH. The solution was transferred to a round-bottom flask, heated in an oil bath at 95 °C for 30 min, and then removed from the heat and allowed to cool. The pH was again adjusted to 7.0, and the heating and pH adjustment was continued until the pH stabilized. The round-bottom flask was then connected to a condenser tube, and the solution was

(17) Kalyanasundaram, K. *Coord. Chem. Rev.* **1982**, *46*, 159.
(18) Davis, W. B.; Ratner, M. A.; Wasielewski, M. R. *J. Am. Chem. Soc.* **2001**, *123*, 7877.
(19) Gust, D.; Moore, T. A.; Moore, A. L. *Acc. Chem. Res.* **2001**, *34*, 40.
(20) Hagfeldt, A.; Grätzel, M. *Acc. Chem. Res.* **2000**, *33*, 269.
(21) (a) van de Lagemaat, J.; Frank, A. J. *J. Phys. Chem. B* **2001**, *105*, 11194. (b) van de Lagemaat, J.; Frank, A. J. *J. Phys. Chem. B* **2000**, *104*, 4292.
(22) Galoppini, E.; Guo, W.; Qu, P.; Meyer, G. J. *J. Am. Chem. Soc.* **2001**, *123*, 4342.
(23) Kaschak, D. M.; Lean, J. T.; Waraksa, C. C.; Saupe, G. B.; Mallouk, T. E. *J. Am. Chem. Soc.* **1999**, *121*, 3435.
(24) Reddington, E.; Sapienza, A.; Gurau, B.; Viswanathan, R.; Sarangapani, S.; Smotkin, E. S.; Mallouk, T. E. *Science* **1998**, *280*, 1735.
(25) Senkan, S. M. *Nature* **1998**, *394*, 350.
(26) Taylor, S. J.; Morken, J. P. *Science* **1998**, *280*, 267.
(27) (a) Copeland, G. T.; Miller, S. J. *J. Am. Chem. Soc.* **1999**, *121*, 4306. (b) Harris, R. F.; Nation, A. J.; Copeland, G. T.; Miller, S. J. *J. Am. Chem. Soc.* **2000**, *122*, 11270.
(28) (a) Cooper, A. C.; McAlexander, L. H.; Lee, D.-H.; Torres, M. T.; Crabtree, R. H. *J. Am. Chem. Soc.* **1998**, *120*, 9971. (b) Crabtree, R. H. *Chem. Commun.* **1999**, *17*, 1611.
(29) Shaughnessy, K. H.; Kim, P.; Hartwig, J. F. *J. Am. Chem. Soc.* **1999**, *121*, 2123.
(30) Yeung, E. S.; Su, H. *J. Am. Chem. Soc.* **2000**, *122*, 7422.
(31) Our attempts to develop amperometric sensors for the direct detection of oxygen in this chemical system failed because of interference from persulfate.

heated for 2 h at 95 °C with oxygen bubbling through it. The $IrO_2 \cdot xH_2O$ colloidal solution was removed from the heat and allowed to cool. The solution was split into two parts: one part was ion-exchanged with chloride-exchanged Dowex 2x8-50 resin, and the other was dialyzed to remove excess citrate ions. The resulting solutions were diluted to twice their initial volumes to make two nominally 6.2×10^{-4} M colloidal $IrO_2 \cdot xH_2O$ solutions.

Parallel Microwave Synthesis of Metal Oxide Colloids. Metal oxide colloids with elemental proportions of Ir_{100} (two duplicates), $Ir_{95}Os_5$, $Ir_{90}Pt_{10}$, $Ir_{90}Ru_{10}$, $Ir_{85}Pt_{10}Os_5$, $Ir_{85}Ru_{10}Os_5$, $Ir_{80}Pt_{20}$, $Ir_{80}Ru_{20}$, $Ir_{80}Pt_{10}Ru_{10}$, and $Ir_{75}Pt_{10}Ru_{10}Os_5$ were prepared. The metal salts used to prepare the metal oxide colloids were K_2IrCl_6, $K_2RuCl_5 \cdot H_2O$, K_2PtCl_4, and $OsCl_3$. Metal salt solutions were prepared by adding enough of the appropriate salt to make the metal concentration 1.55×10^{-3} M in a 4.75×10^{-3} M sodium hydrogen citrate sesquihydrate solution. The pH of each solution was adjusted to 7.0 using 0.25 M NaOH. Different colloid compositions were made by using metal salt solutions in the correct proportions to make 20 mL total. Five milliliters of a 1.05×10^{-2} M Na_2CO_3 solution was added to each reaction tube. The reaction solutions with varying proportions of Ir:Pt:Ru:Os were heated simultaneously in a MARS5 (CEM Corp., Matthews, NC) microwave digestion system at 95 °C for 2 h. The metal oxide colloid solutions were then cooled to room temperature and dialyzed separately to remove excess citrate ions. The volumes were diluted to 50 mL each to make 6.2×10^{-4} M (based on total metal) metal oxide colloidal solutions. The solutions were then filtered through a 0.2 μm filter so that they would not clog the tip of the robotic plotter used to dispense reagents into multiwell plates for screening.

Serial Testing of Oxygen Evolution Catalysis. Typical reaction conditions were the same as those described by Hara et al.[16] The concentrations of $Ru(bpy)_3^{2+}$, metal oxide colloid, Na_2SO_4, and $Na_2S_2O_8$ were 1.1×10^{-4}, 6.2×10^{-5}, 0.05, and 0.01 M, respectively. The buffer was made by taking 3.75×10^{-2} M Na_2SiF_6 and adding enough $NaHCO_3$ to make the pH 5.7. The concentration of $NaHCO_3$ in the buffer solution was approximately 8.0×10^{-2} M. The buffer solution was sonicated for 15 min and aged overnight. The aging step was important since the actual buffer is a poly(silicate) hydrolysis product of Na_2SiF_6. The buffer was filtered, and 2.9 mL was added to the reaction solution along with the other reagents for a total of 5 mL of reaction solution. The reaction solution was put in a sealed 26 mL test tube. The test tube was placed in an outer vessel with argon flowing through it to prevent contamination by air. After the solution was purged with argon for 15 min, it was irradiated with light from a 450 W Xe/Hg lamp filtered by a 450 nm bandwidth filter for the initial and optimized experiments, and by a 420 nm cutoff filter for the microwave experiments. Gas samples were removed from the test tube as the reaction proceeded and analyzed for oxygen content by GC using a thermal conductivity detector and room-temperature molecular sieve 5A columns (Supelco).

High-Throughput Testing of Catalyst Arrays. Unless otherwise noted, the same concentrations of reagents were used as in the serial oxygen evolution studies. Reagent aliquots were distributed into a 96-well plate either by hand pipetting or by means of a robotic plotter (Cartesian Technologies, PixSys 3200). The well plates were irradiated on a Horizon 2 16000 Series (Apollo) overhead projector, and absorbance and emission scans were done intermittently throughout the course of the photolysis using an HTS 7000 Plus Bio Assay Reader (Perkin-Elmer). The plate reader required approximately 25 s to measure a 96-well array, after which it was returned to the overhead projector. The light intensity from the overhead projector was highest at the center (where the 96-well plate was placed) and varied about 25% between the center and edges of the plate. Multiple samples (typically three or four) were used for each composition and were randomly placed in the array to compensate for variations in light intensity. The reported absorbance readings represent an average of those measurements. The standard deviation of the parallel screening method, obtained from the variances of 67 such averages, was 0.021 absorbance unit, or about 6−10% of a typical absorbance value.

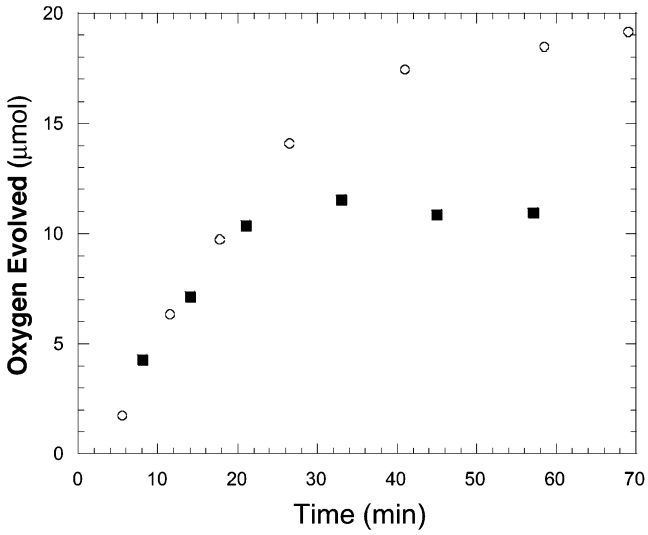

Figure 1. Photochemical oxygen evolution using $IrO_2 \cdot xH_2O$ colloids with the excess citrate removed by ion exchange (■) and by dialysis (○).

Results and Discussion

Proof-of-Concept Testing of the Optical Screening Method. To test the viability of the high-throughput optical screening method, $IrO_2 \cdot xH_2O$ was prepared by conventional convection heating, with the excess citrate ions being removed by either ion exchange or dialysis. Figure 1 shows plots of oxygen evolution vs time for these catalysts. At early times, the reaction rate is light-limited, and the apparent rate is the same for both catalysts. However, after about 20 min the plots diverge, and eventually both curves level off as the sensitizer is progressively destroyed. As shown in Figure 1, the ion-exchanged colloid produced slightly more than half the oxygen as the dialyzed colloid under the same conditions. UV−visible spectra showed that the ion-exchanged colloid had only 44% of the absorbance of the dialyzed colloid at 580 nm, indicating that much of the colloid was lost during the synthesis by adsorption to the ion-exchange resin. These two colloidal catalyst solutions provided benchmark "good" and "bad" catalysts for testing the optical screening method.

Using similar reaction solutions in 96-well plates, a series of 16 wells were irradiated and tested. Each lane contained four identical solutions: one set each of a solution with no colloid, the "bad" ion-exchanged colloid, the "good" dialyzed colloid, and one solution containing no sacrificial acceptor. In these experiments, the wells containing no colloid were expected to show the most rapid decomposition of the sensitizer, and those with no sacrificial acceptor were expected to show little or no decomposition. The "good" and "bad" catalysts represent intermediate cases, in which the oxygen evolution cycle is kinetically competitive with $Ru(bpy)_3^{3+}$ decomposition.

As seen in Figure 2A, the 430 nm absorbance of the samples with no colloid decreased abruptly, followed by the absorbance of samples with the ion-exchanged colloid. $Ru(bpy)_3^{2+}$ was present in the sample with the dialyzed colloid for a longer amount of time. In this experiment, the "good" and "bad" catalysts are differentiated after about 10 min, and the absorbance of the "bad" catalyst reaches a baseline level after about

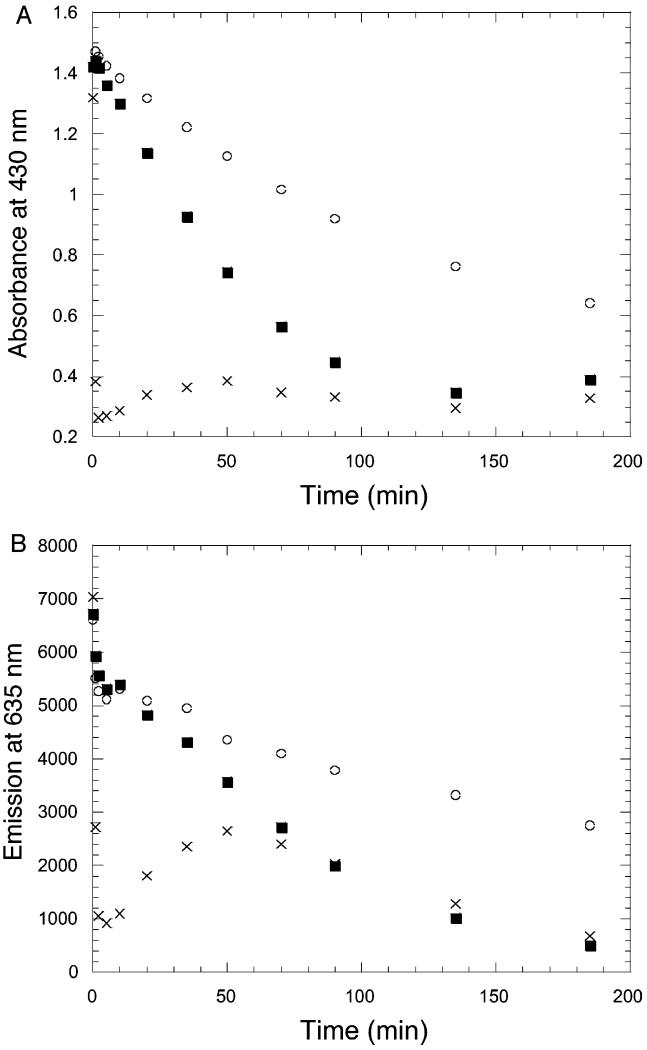

Figure 2. (A) Absorbance at 430 nm of reaction solutions with no colloid (×), ion-exchanged colloid (■), and dialyzed colloid (○) vs irradiation time and (B) the emission (excitation at 430 nm and emission at 635 nm) of reaction solutions with no colloid (×), ion-exchanged colloid (■), and dialyzed colloid (○) vs irradiation time.

2 h. The ranking of catalytic activity is the same as that shown in Figure 1; however, the difference is not apparent at early times in Figure 1 because the oxygen evolution rate is light-limited. Emission measurements were also taken, using an excitation wavelength of 430 nm and an emission wavelength of 635 nm as shown in Figure 2B. The emission plots are consistent with more rapid decomposition of the sensitizer in the presence of the "bad" ion-exchanged colloid. However, the rapid decay and reappearance of an emission signal in the "no colloid" sample shows that some emissive products are formed in the complex decomposition pathway of $Ru(bpy)_3^{3+}$.[32] Finally, the same rank ordering of catalysts could be observed in emission snapshots of the array (Figure 3). Initially, all the wells show bright fluorescence, but the sensitizer is destroyed within 3 min in the lane with no colloid. The "good" and "bad" catalysts are easily differentiated from the control lanes, but not from each other, after 40 min of irradiation. This is quite consistent with the results shown in Figure 2B.

Optimization of Reaction Conditions. The parallel screening method was first used with a single $IrO_2 \cdot xH_2O$ colloid to identify the optimal reaction conditions for oxygen evolution. Factors

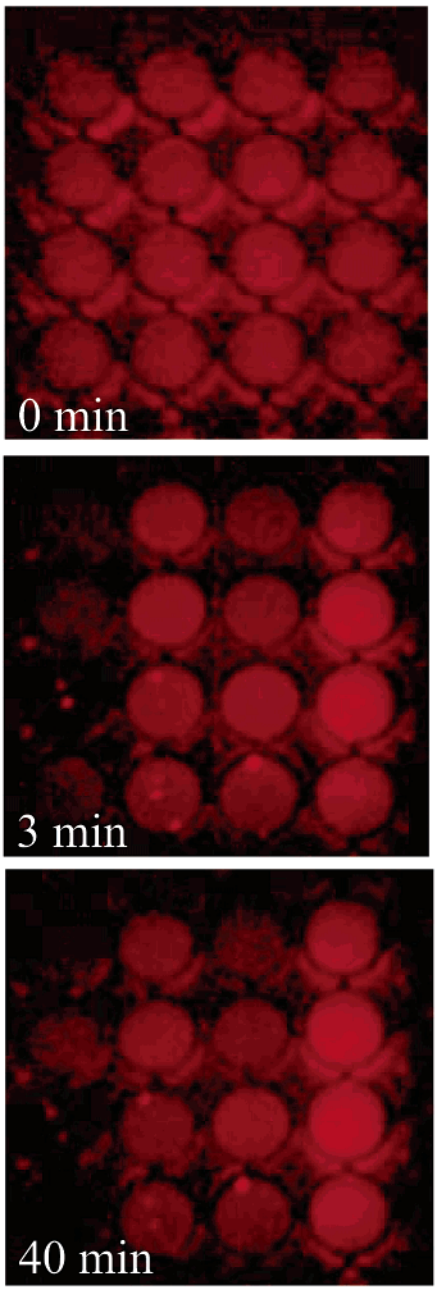

Figure 3. Emission snapshots of a well plate containing sensitizer−colloid−sacrificial acceptor reaction solutions: lane 1, no colloid; lane 2, ion-exchanged colloid; lane 3, dialyzed colloid; and lane 4, no sacrificial acceptor. Conditions were the same as those used in Figure 2. The emission images were aquired through a red filter by illuminating with 450 nm light.

that could be optimized easily using this method included the $Ru(bpy)_3^{2+}$, colloid, and added Nafion concentrations, as well as the buffer pH. It was found in a preliminary screening study that the sulfate and buffer concentrations had little effect on the absorbance response of the $Ru(bpy)_3^{2+}$ sensitizer.

With the aid of JMP Statistical Discovery Software (SAS Institute), an orthogonal central composite design of experiments was chosen to test these four factors. In an orthogonal central composite design (CCD), five levels (values) for each factor (concentration or pH) are studied in different combinations, allowing a response surface to be modeled effectively, even if

(32) Ghosh, P. K.; Brunschwig, B. S.; Chou, M.; Creutz, C.; Sutin, N. *J. Am. Chem. Soc.* **1984**, *106*, 4772.

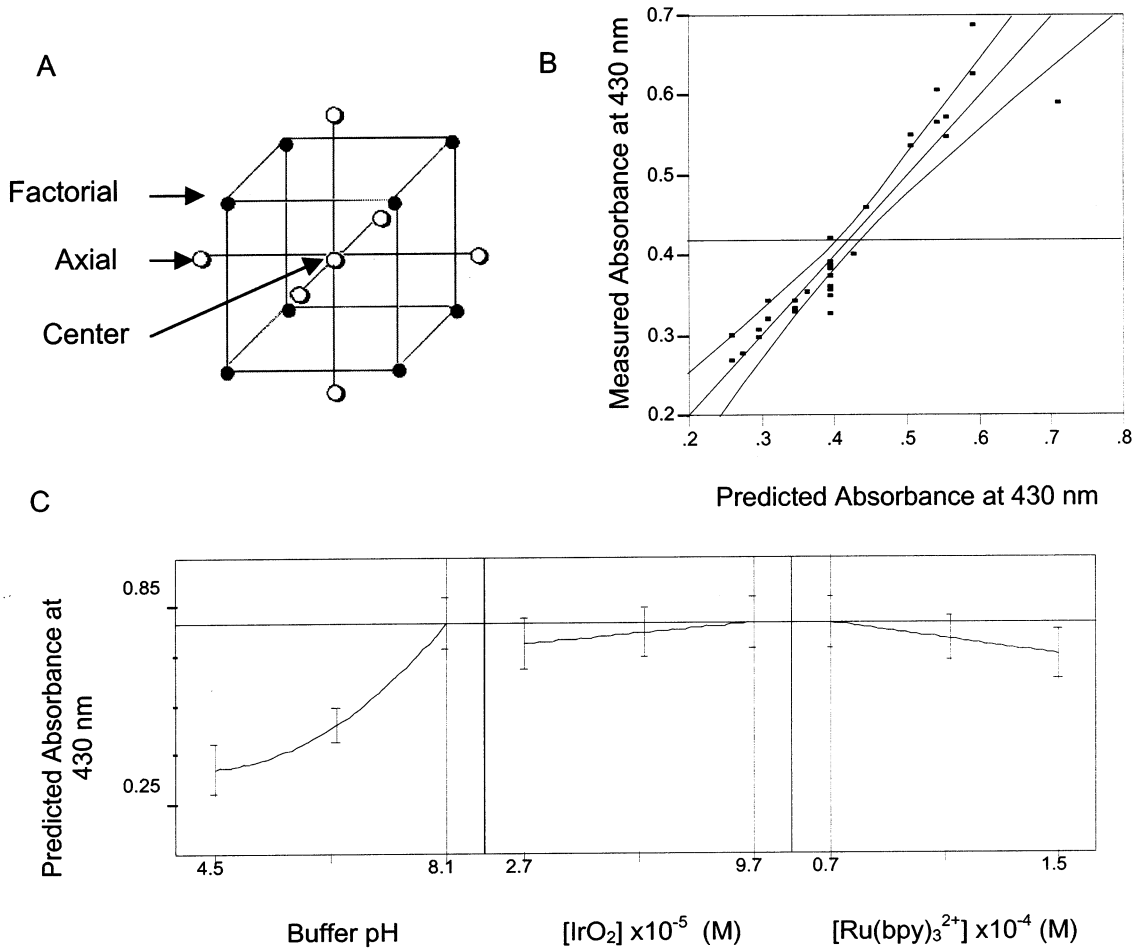

Figure 4. (A) Three-factor orthogonal central composite design (CCD) of an experiment in which each axis corresponds to a factor, the center point represents an average value for each factor, and the circles represent the values at which the experiment is conducted. (B) Plot of experimental absorbance values after 30 min of irradiation vs absorbance predicted from a least-squares fit to the four-factor orthogonal CCD data. The horizontal line indicates the average response, and the curved lines on either side of the best-fit line show the 95% confidence interval. (C) Contour profiles of the response surface showing the factor levels that give the maximum predicted absorbance (vertical lines). Error bars show the 95% confidence interval.

the response is nonlinear or has strongly interacting parameters.[33] An orthogonal CCD for three factors is shown schematically in Figure 4A.[34] The number of factorial points amounts to 2^k, where k is the number of factors. There were 16 factorial points in the four-factor design for this series of experiments. Factorial points test high and low values for each factor in all possible combinations. Axial points test a high or low extreme value for one factor while the remaining factors are held at an average value. The number of axial points is $2k$, or eight in this experiment. Finally, several replicate experiments are done at the central point, an average value for all factors. Seven replicate experiments were performed using the central point conditions.

These 31 sets of reaction conditions were tested in triplicate in a 96-well plate, and average absorbance values were used in the calculations that generated the response surface. The levels of each factor tested were the following: colloid concentration, $(2.7-9.7) \times 10^{-5}$ M $IrO_2 \cdot xH_2O$; Nafion concentration, 0−0.05 g/L; $Ru(bpy)_3^{2+}$ concentration, $(0.75-1.45) \times 10^{-4}$ M; and buffer pH, 4.5−8.1. The number of moles of $Ru(bpy)_3^{2+}$ in each well was held constant, even though the concentrations were different, meaning that different wells contained different volumes of reaction solution. Because the amount of $Ru(bpy)_3^{2+}$ was constant, the initial absorbance was comparable for all wells. The buffer and sacrificial acceptor concentrations were held constant in each well. Absorbance data were acquired, and the averaged data at 30 min irradiation time (where the absorbance values of samples in the array were well differentiated) were used to calculate the response surface.

From the array absorbance data, an initial polynomial least-squares fit to the response surface was generated in the form

$$y = b_0 + b_1x_1 + b_2x_2 + b_3x_3 + b_4x_4 + b_{11}x_1^2 + b_{22}x_2^2 + b_{33}x_3^2 + b_{44}x_4^2 + b_{12}x_1x_2 + b_{13}x_1x_3 + b_{14}x_1x_4 + b_{23}x_2x_3 + b_{24}x_2x_4 + b_{34}x_3x_4 \quad (1)$$

Here, y is the absorbance and b_i is the coefficient for the ith factor, x_i. This equation allows for single-parameter and two-parameter cross terms in the response surface but neglects higher order interactions. An intial 15-parameter fit to the 31 independent data points yielded an R^2 value of 0.92. However, it was found that the addition of Nafion, within this concentration range, had no significant effect on the absorbance values. This

(33) *JMP Design of Experiments, Version 4*; SAS Institute: Cary, NC, 2000; p 74.

(34) Figure adapted from: Langhans, I. Designs for Response Surface Modelling−Quantifying the Relation Between Factors and Response. In *Design and Analysis in Chemical Research*; Tranter, R. L., Ed.; CRC Press: Boca Raton, FL, 2000; p 250.

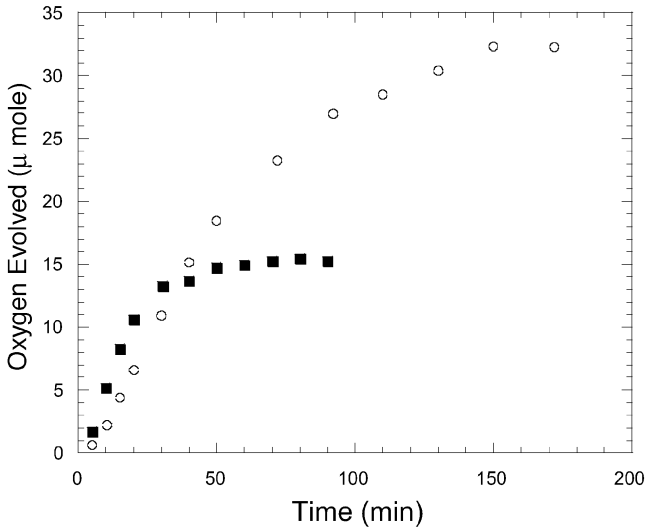

Figure 5. Oxygen evolution data testing the performance of a conventional IrO_2 colloid under original (■) and optimized (○) conditions.

parameter and the relevant cross terms were left out of the final fit. Additionally, most of the other cross terms were found to be insignificant within the margin of error of the data. The final least-squares fit included only five coefficients: three single-factor terms, one quadratic term (pH), and a baseline value, b_0. The final response surface had the form

$$y = b_0 + b_1(\text{buffer pH}) + b_2[\text{Ru(bpy)}_3^{2+}] + b_3[\text{IrO}_2] + b_{11}(\text{buffer pH})^2 \quad (2)$$

The correlation between the fit and the experimental absorbance at 30 min is shown in Figure 4B. The R^2 value is 0.89, indicating a good correlation between the absorbance data and that predicted from eq 2. Figure 4C shows a contour profile of the response surface along each of the variable axes and indiates that the best conditions within the range tested represent the high values of pH and colloid concentration, and the low value $Ru(bpy)_3^{2+}$ concentration. A higher absorbance of the solution indicates a longer lifetime of the $Ru(bpy)_3^{2+}$ sensitizer during the reaction. Barring any great differences in the rate of the $Ru(bpy)_3^{3+}$ decomposition reaction, this implies a higher number of turnovers for these reaction conditions.

Oxygen evolution tests were performed under both the original conditions (Figure 1) and the optimized conditions obtained by analysis of the absorbance data. Optimal concentrations tested were 0.7×10^{-4} M $Ru(bpy)_3^{2+}$, 1.0×10^{-4} M metal oxide colloid, 0.05 M Na_2SO_4, and 0.010 M $Na_2S_2O_8$. The buffer was made by taking 3.75×10^{-2} M Na_2SiF_6 and adding enough $NaHCO_3$ to make the pH 6.7. The buffer solution was sonicated for 15 min, and the pH was rechecked. After sonication, the pH increased considerably. If the pH was lower than 8.1, more $NaHCO_3$ was added, and the buffer was again sonicated. If the pH was too high, 3.75×10^{-2} M Na_2SiF_6 was added to adjust to the correct pH. The buffer was filtered and aged for 3 h, and 4.55 mL of buffer was added to the reaction solution along with the other reagents for a total of 7.86 mL of reaction solution. The larger volume was needed to retain the same number of moles of $Ru(bpy)_3^{2+}$ as was in the reaction under the original conditions. Figure 5 shows a 2-fold increase in number of turnovers using these optimized conditions. It should be noted that the initial (light-limited) rate of oxygen evolution is lower, because less light is absorbed by the more dilute sensitizer solution; however, the total amount of oxygen evolved is greater. Under the optimized conditions (where the pH is considerably higher), the colloid also flocculates midway through the reaction but continues to evolve oxygen photochemically.

Table 1. Number of $Ru(bpy)_3^{2+}$ Turnovers for 10 Different Colloid Compositions Calculated from Oxygen Evolution Data and from Absorbance Measurements from the 96-Well Plate after 22 min of Irradiation

metal oxide colloid metal composition	no. of $Ru(bpy)_3^{2+}$ turnovers	absorbance at 430 nm after 22 min of irradiation
$Ir_{85}Pt_{10}Os_5$	145	0.405
$Ir_{95}Os_5$	144	0.398
$Ir_{90}Pt_{10}$	138	0.371
$Ir_{80}Pt_{20}$	135	0.374
Ir_{100} a	127	0.352
Ir_{100} b	125	0.322
$Ir_{80}Pt_{10}Ru_{10}$	123	0.300
$Ir_{75}Pt_{10}Ru_{10}Os_5$	122	0.374
Ir_{100} c	122	0.361
$Ir_{90}Ru_{10}$	114	0.266
$Ir_{85}Ru_{10}Os_5$	110	0.257
$Ir_{80}Ru_{20}$	86	0.251

Optimization of the Catalyst Composition. The availability of a rapid screening method opens the possibility of testing colloid compositions beyond simple binary oxides. Because $IrO_2 \cdot xH_2O$ is known to be the best of these oxides, we investigated compositions containing primarily Ir with small added amounts of other transition elements. Pt, Ru, and Os were chosen because together they have been found to give good electrochemical water oxidation catalysts.[35] These dopants were used in small quantities so that the same preparation method could be used for each colloid. Colloid preparation by microwave heating was chosen because it presented advantages of speed and parallel synthesis, although in general it gave catalysts that were inferior to those produced by the convective heating method. Identical heating cycles were ensured since all samples could be prepared simultaneously in one batch.

Twelve different colloid compositions were chosen, and both serial oxygen evolution tests and parallel optical screening were performed. It should be noted that the highest reported number of turnovers for this reaction, using colloids made by convection heating, is about 290, corresponding to 40 μmol of O_2 evolved.[16] Under similar conditions, 125 turnovers are more typical with microwave colloids. The number of $Ru(bpy)_3^{2+}$ turnovers was calculated by taking the moles of oxygen evolved multiplied by 4 and divided by the moles $Ru(bpy)_3^{2+}$ used. Four turnovers of $Ru(bpy)_3^{2+}$ corresponds to one oxygen molecule, as shown in the following reaction sequence:[15]

$$\text{Ru(bpy)}_3^{2+} + h\nu \rightarrow \text{Ru(bpy)}_3^{2+*} \quad (3)$$

$$\text{Ru(bpy)}_3^{2+*} + \text{S}_2\text{O}_8^{2-} \rightarrow \text{Ru(bpy)}_3^{3+} + \text{SO}_4^{2-} + \text{SO}_4^{-} \quad (4)$$

$$\text{Ru(bpy)}_3^{2+} + \text{SO}_4^{-} \rightarrow \text{Ru(bpy)}_3^{3+} + \text{SO}_4^{2-} \quad (5)$$

$$4\text{Ru(bpy)}_3^{3+} + 2\text{H}_2\text{O} \rightarrow 4\text{Ru(bpy)}_3^{2+} + 4\text{H}^+ + \text{O}_2 \quad (6)$$

The numbers of turnovers obtained using the various colloids are shown in Table 1 and are plotted in Figure 6, along with

(35) Chen, G.; Delafuente, D. A.; Sarangapani, S.; Mallouk, T. E. *Catal. Today* **2001**, *67*, 341.

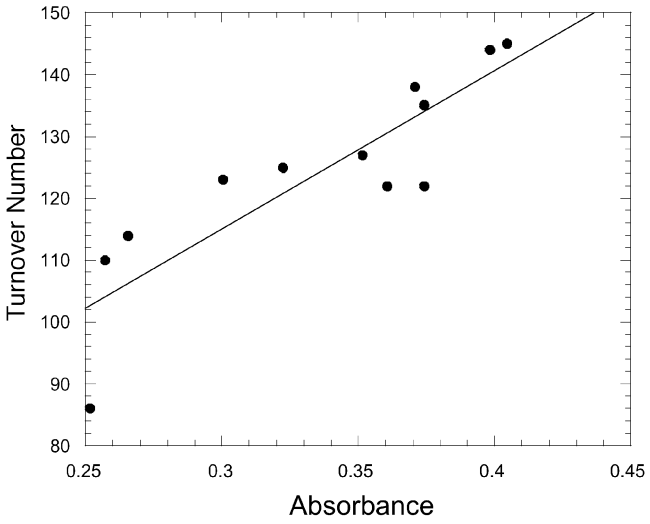

Figure 6. Correlation between number of $Ru(bpy)_3^{2+}$ turnovers and absorbance measurements.

absorbance values taken from the plate reader at 22 min. After 22 min of irradiation (approximately midway through the reaction), the highest and lowest absorbance values were best separated. The correlation coefficient relating the two was 0.87. There are several factors that could negatively affect this correlation. If a given colloid accelerates the decomposition of adsorbed $Ru(bpy)_3^{3+}$ ions, then the number of turnovers would be low even if the oxygen evolution rate is high. Another factor is the absorbance of the colloid itself, since additives such as ruthenium make the colloids darker than those that contain only iridium. Despite these factors, it appears that the high-throughput method is well correlated with the oxygen evolution rates of different colloids.

In Figure 7, the variation in number of turnovers with the metal dopant concentration is evident. Colloids containing Os and Pt dopants are more active than those containing only Ir, and those with Ru are less active. Because the area of highest activity in the initial screening of these four metals was found at the upper limit of osmium and platinum used, a second experiment was done to examine the Ir−Pt−Os ternary compound more completely. The response surface obtained by ranking 21 compositions (Figure 7) shows a single optimal region within this ternary composition diagram at ca. 5% Os and 30−50% Pt. TEM images of selected colloids from these experiments showed that the most active Pt- and Os-containing colloids contained uniform particles with diameters in the 10−15 nm range, whereas those without these elements had larger particles. This suggests that the primary effects of these "dopants" is to increase the number of surface Ir atoms

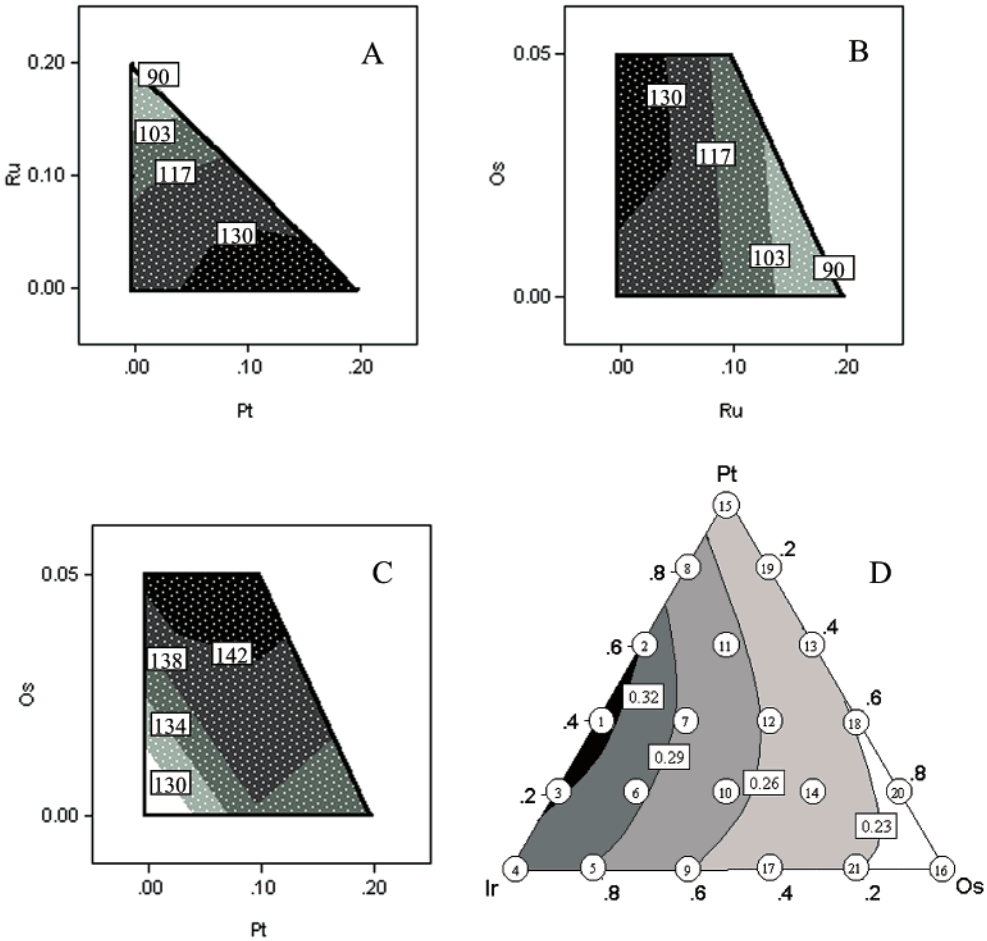

Figure 7. (A−C) Contour plots showing the effects of Pt, Ru, and Os dopants at low concentrations. Contour lines along the axes show the single-factor effect of each dopant on the number of turnovers. Contour lines along the diagonals illustrate the two-factor interactions. The JMP software used a method of triangulation and linear interpolation to construct the contour plots from the number of turnovers given in Table 1. The triangle in (D) ranks 21 photocatalysts in the Ir−Pt−Os ternary compound at higher levels of Pt and Os. Contour lines indicate absorbance values after 8 min of irradiation, and numbers in circles show the absorbance ranking of each composition.

available for catalysis. These observations are worthy of further study in the search for a better water oxidation catalyst. Other metals performing well in Harriman's experiments as powders that could also be tested as additives include Rh, Mn, and Co.[13]

The bottleneck that prevents this optical screening method from broad-range combinatorial screening of catalyst compositions is the preparation and dialysis of the colloidal catalysts. The microwave preparation method used here reduces preparation time substantially: the per-colloid preparation time is about 15 min (when 14 colloids are made in parallel), compared to 5 h for the conventional convective heating approach. Unfortunately, the average particle diameter of $IrO_2 \cdot xH_2O$ prepared by the microwave method is about 50 nm, and therefore the particles have relatively low activity. The dialysis process is also unwieldy for combinatorial synthesis, although again this step can be done in parallel. Using the design-of-experiment approach, it is possible to optimize reaction conditions and compositions using a minimum number of unique samples. Thus, it should be possible to combine parallel synthesis, design of experiments, and optical screening in an iterative manner to test a wide range of catalyst compositions.

Conclusions

The parallel optical screening method, combined with reaction surface modeling, has proven effective in optimizing the conditions for photocatalytic oxygen evolution. Perhaps the most surprising finding from this study is that relatively basic solutions (pH 8) give higher numbers of turnovers than those at pH 5−6, at which the reaction has previously been optimized.[16] Although the driving force for oxygen evolution from $Ru(bpy)_3^{3+}$ increases at higher pH, one expects that the rate of nucleophilic attack by OH^- (see Scheme 1) should also increase. Measurements of $Ru(bpy)_3^{3+}$ decomposition, using methanol to reduce photogenerated Ru^{3+} as described in ref 16, give first-order rate constants of $1.34(2) \times 10^{-3}$ and $8.25(3) \times 10^{-4}$ s^{-1} at pH 5.7 and 7.6, respectively. This shows that the increase in number of turnovers at higher pH is due predominantly to a decreased decomposition rate, rather than an increased oxygen evolution rate at the colloid surface.

The screening method has also led to the discovery of doped $IrO_2 \cdot xH_2O$ colloids with moderately improved catalytic activity. In general, these microwave-prepared colloids have lower activity than those made by convective heating, but the enhancement found with Pt and Os dopants is interesting. A good correlation was found between the number of $Ru(bpy)_3^{2+}$ turnovers calculated from the oxygen evolution data and the absorbance readings obtained using the screening method. This suggests that the method could be useful in examining a broader range of catalyst compositions, provided that sufficiently high-throughput synthetic methods can be developed.

Finally, we note that a wide range of photocatalytic systems (involving zeolites, vesicles, clays, semiconductor nanoparticles, and other organizing media) use $Ru(bpy)_3^{2+}$ and its derivatives as photosensitizers. In principle, this high-throughput optical method could be adapted to the optimization of many of those systems by introducing a decomposition reaction (such as nucleophilic attack, as used here, or photoanation by halide ions) that competes kinetically with the photocatalytic cycle.

Acknowledgment. We thank the Division of Chemical Sciences, Office of Basic Energy Sciences, U.S. Department of Energy, for their support under Contract DE-FG02-93-ER14374. We also thank Dr. Bharat L. Newalker and Prof. Sridhar Komarneni from the Materials Research Laboratory at Pennsylvania State University for assistance with and use of their microwave digestion system.

JA017895F